Chemical Engineering Journal 152 (2009) 471–479

Contents lists available at ScienceDirect

Chemical Engineering Journal

journal homepage: www.elsevier.com/locate/cej

The influence of polymeric dispersants on sericite–chalcocite particle interactions in aqueous media

Mingzhao He, Jonas Addai-Mensah*, David Beattie

Ian Wark Research Institute, University of South Australia, Mawson Lakes, SA 5095, Australia

ARTICLE INFO

Article history:
Received 13 October 2008
Received in revised form 27 April 2009
Accepted 8 May 2009

Keywords:
Hetero-aggregation
Particulate adsorption
Particle zeta potential
Polymeric dispersant
Shear rheology
Mix silicate–copper sulphide minerals

ABSTRACT

Unexpected sericite–chalcocite mineral particles' hetero-aggregation occurs under aqueous processing conditions where both minerals display negative zeta potentials. In this study, the use of anionic co-polymers (carboxylate- versus sulphonate-substituted) as dispersants to suppress the hetero-aggregation behaviour was investigated in the pH range 5–9. Both polymers showed strong substrate and pH-dependent adsorption and electrokinetic potential characteristics onto both minerals. The adsorption propensity was considerably higher onto chalcocite than sericite particles and dramatically accentuated at pH 5 for the former due to leached electropositive Cu(II) species' surface activation effect. At high polymer dosages (>1.5 g kg^{-1} solid) leading to plateau adsorption density, the magnitude of both mineral particles' zeta potential increased to a maximum. Furthermore, the adsorbed polymer layer dominated the interfacial chemistry that showed subtle mineral phase and pH dependency. The concomitant particle interactions reflected a marked reduction of dispersion shear yield stress and the suppression of sericite–chalcocite particulate adsorption. Electro-steric repulsive forces are believed to be responsible for the dispersing mechanism. Both polymers displayed similar, high dispersing efficacy at dosages >1.5 g kg^{-1} solid for sericite–chalcocite mix dispersions, regardless of the pH.

1. Introduction

During hydrometallurgical processing of liberated valuable sulphide ores (e.g., chalcocite), hydrophilic silicate clay gangue minerals (e.g., sericite) often associate with the former, reducing its hydrophobicity. Furthermore, gangue-value minerals' hetero-aggregation or "sliming" can also reduce flotation collector's adsorption selectivity [1–5]. The incidental flotation depression mechanisms have deleterious impact on valuable minerals' floatability, flotation rate and recovery [5–7]. Slime coating of value minerals may occur through several, attractive particle interaction mechanisms (e.g., electrostatic, van der Waals, charge patch attraction, hydrophobic, and ion-bridging forces) [1,3,5,8–12]. Undesirable value sulphide–waste minerals association not only leads to increased metal concentrate smelting costs with significant economic losses to the minerals industry, but also poses an environmental cleaning challenge. Waste tailings comprising sulphide minerals must be adequately treated to minimize the acid rock drainage effect they impart to the environment.

A number of methods are employed to prevent the occurrence of hetero-aggregation between clay slimes and sulphide minerals. They include high intensity conditioning [9,10], pH modification and nitrogen gas purging [12] and dispersant addition [1,8,13,14]. Charged, low molecular weight (e.g., $<5 \times 10^4$ Da) polymers are typically used as dispersants to control and prevent mix mineral phase–particulate attraction during grinding, pulp conditioning or flotation. The adsorption of a polyelectrolyte onto mineral particles often causes an increase in the magnitude of the particle zeta potential and/or even result in charge reversal [1,8,13,14]. The resulting gangue or valuable mineral electrokinetic potential modification may then change the particle interactions from attraction to repulsion. The electrostatically or electro-sterically repulsive forces that invariably emerge, thus, prevent hetero-aggregation between the particles.

In the present work, hetero-aggregation or sliming and its mitigation of sericite and chalcocite minerals, commonly occurring in gangue and valuable sulphide minerals, respectively, are of interest. Sericite is a hydrophilic fine-grained mica with layered alumino-silicate structure. Its elementary sheet is composed of a layer of alumina octahedral sandwiched between two silica tetrahedral layers, of which the components are linked by ionic and covalent bonds. Chalcocite is a reactive Cu(I) sulphide mineral. It may oxidize and leach Cu(II) species once it is in contact with water containing dissolved molecular oxygen at moderate to low pH, even at room temperature [15–17]. In the pH range 5–9 within which the present investigations were undertaken, it has

* Corresponding author. Tel.: +61 8 83023673; fax: +61 8 83023683.
E-mail address: jonas.addai-mensah@unisa.edu.au (J. Addai-Mensah).

1385-8947/$ – see front matter.
doi:10.1016/j.cej.2009.05.010

recently been shown that sericite particles hetero-aggregated with chalcocite particles dispersed in 0.01 M KNO_3 electrolyte under air-saturation [12]. The mix phase hetero-aggregation was contrary to expectation as both sericite and chalcocite mineral particles were negatively charged, according to their apparent particle zeta potentials. Further investigations showed that the unexpected particulate attraction correlated strongly with chalcocite oxidation and leaching of Cu(II) species that hydrolyzed and specifically adsorbed onto both mineral phases [12]. The corresponding interfacial chemistry change led to increased, attractive particle interactions under high shear rate conditions, in the manner of mechanisms such as strong electrostatic/charged patch attraction, ion particle bridging, surface nucleation and cementation and enhanced van der Waals attraction. Whilst the introduction of N_2 gas into the suspension and pulp conditioning at high pH values (>7) significantly reduced the sliming behaviour, they did not completely eliminate it [12]. In the quest of a more cost-effective sliming mitigation strategy, selected synthetic polymers may be examined as dispersing aids.

In this work, the use of two, low molecular weight, anionic polymeric dispersants to modify pulp interfacial chemistry and mediate sericite–chalcocite particle interactions in aqueous dispersions for effective sliming mitigation was investigated at pH 5, 7 and 9. The two polymers were carboxylate-substituted polyacrylamide and sulphonate-substituted polymaleic acid co-polymers. Both polymers with pKa of 4.2–4.6 begin to dissociate and become anionic at pH > 2. Pulp/interfacial chemistry was quantified via solution speciation, polymer adsorption and particle zeta potential analyses. Particle interactions were probed through continuous flow sericite–chalcocite particulate adsorption and shear rheology studies as a function of dispersion conditions. The particulate adsorption experiment provides direct, visual and valuable information on the mixed mineral particle interactions: sliming and dispersion behaviour.

2. Materials and experimental

2.1. Materials

High purity chalcocite (Cu_2S, >98% purity with 1.21% Cl and 0.56% Fe; Ward's Natural Science Establishment Inc., USA) with a density of 5650 kg m^3 and sericite ($K_{0.91}Na_{0.07}(Al_{1.82}Fe_{0.14}Mg_{0.08})(Al_{0.93}Si_{3.07}O_{10})(OH)_2$, >99% purity with traces of Ca and Mg impurities; IKEDA Co., Japan) with a density of 2800 kg m^3 were used. The Cu_2S sample was first dry ground using a laboratory Fritsch vibrational mill, and the product classified by dry sieving through a 45-μm aperture (Endecotts Ltd., England). The <45-μm size fraction with a BET-specific surface area of 0.68 m^2 g^{-1} and D_{10}, D_{50}, and D_{90} sizes of 7.1, 15.6 and 40.5 μm, respectively, was used for rheological measurements and solution Cu(II) species–polymer interaction studies. Large (~1.5 cm × 1.0 cm × 1.0 cm) chalcocite particles with polished planar surfaces were used in the particulate adsorption studies. Smooth polishing of the particles was performed using colloidal/nano-alumina particles (0.3 and 0.015 μm) on Buehler polishing cloths. For colloidal chalcocite particle zeta potential measurements, 1.5 g of the sample was dry ground using a ceramic mortar and pestle, then dispersed and homogenized at pH 11 in 0.01 M KNO_3 just prior to measurements. Sericite sample used had a BET-specific surface area of 8.8 m^2 g^{-1} with D_{10}, D_{50}, and D_{90} sizes of 2.2, 9.7 and 34.7 μm, respectively. To eliminate the possible effect due to surface contamination, the sericite powder samples were first conditioned at pH 3 for 1 h by washing in 0.01 M KNO_3 electrolyte under an agitation rate of 300 rpm. The washing process was repeated twice, followed by a final dispersion in fresh 0.01 M KNO_3 solution, prior to use.

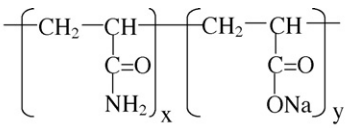

Cyquest 3223

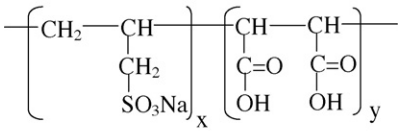

P80

Fig. 1. Structures of carboxylate-substituted polyacrylamide (Cyquest 3223) and sulphonate-substituted polymaleic acid (P80) co-polymers, where *x* and *y* denote the monomer molar ratios of ~4:1.

The properties and structures of the anionic carboxylate-substituted polyacrylamide (Cyquest 3223) and sulphonate-substituted polymaleic acid (P80) co-polymers (Cytec industries, USA) used as dispersants are given in Table 1 and Fig. 1, respectively. Analytical reagent grade potassium nitrate (KNO_3), cupric nitrate ($Cu(NO_3)_2{\cdot}2.5H_2O$), nitric acid (HNO_3) and potassium hydroxide (KOH) (Chem-Supply Pty. Ltd., Australia) were used in solution preparation and pH modification. High purity water (pH ~5.5, surface tension of 72.8 mN m^{-1} and electrical conductivity of 50 μS cm^{-1}) was employed in solution and suspension preparation. All experiments were performed at room temperature (23 °C), unless otherwise stated.

2.2. Experimental

2.2.1. Continuous flow particle–particle adsorption

Sericite–chalcocite particle interactions and the efficacy of polymer-mediation of the process were directly probed using a continuous flow particulate adsorption cell. Full details of the cell, particulate adsorption measurements and data analysis are well described elsewhere [12]. The experiments involved continuous metering of pre-conditioned, 3.5 wt.% solid sericite suspensions at a linear flow and shear rate of 76.2 mm s^{-1} and 600 s^{-1}, respectively, over a polished, planar chalcocite surface immobilized centrally in the base of the cell. The particulate adsorption kinetics behaviour was quantified as a percentage of the chalcocite surface area covered by sericite particles as a function of time through captured microscopic images.

2.2.2. Polymer adsorption

Polymer adsorption was characterized using total organic carbon (TOC) analysis and the depletion method. 5 wt.% solid sericite and chalcocite suspensions were prepared in 0.01 M KNO_3 solution under air-saturated conditions and homogenized by magnetic stirring for 30 min at the pristine pH ~5.5 and ~6, respectively. The suspension pH was then adjusted to a desired value and further stirred for 10 min. 1 g dm^3 stock Cyquest 3223 and P80 polymer solutions in 0.01 M KNO_3 were prepared and also homogenized by magnetic stirring at the pristine pH 8.7 and 3.4, respectively, overnight. Prior to use, the Cyquest 3223 or P80 polymer solution pH was adjusted to a desired value and magnetically stirred for 30 min. A known amount of the mineral suspension was then mixed with a required volume of polymer solutions to obtain 3.5 wt.% solid sericite or chalcocite suspensions at different polymer dosages. The resulting suspensions were then mixed for 2 h using a rotary mixer, and thereafter centrifuged over 10 min at 10,000 rpm. The supernatants were used for TOC analysis to determine solution polymer

Table 1
Properties of both Cyquest 3223 (carboxylate-substituted polyacrylamide) and P80 (sulphonate-substituted polymaleic acid) polymers.

Polymer	Mn (g mol^{-1})	Mw (g mol^{-1})	PD	Main and effective component	Density (g cm^{-3})	pKa
Polymer Cyquest 3223	8600	26,000	3.0	Sodium acrylate/acrylamide co-polymer	1.3	4.2
Polymer P80	5000	8,500	1.7	Sodium allyl sulphonate/maleic acid co-polymer	1.33	4.6

concentration. It was assumed that the amount of polymer depleted from solution was equivalent to that adsorbed onto the mineral particle surface. The adsorbed polymer density (Γ) was then calculated as [18,19]:

$$\Gamma = \frac{1}{mA_s}(c_i - c_f)V \quad (1)$$

where m and A_s are the mass and the specific surface area of the solid substrate, respectively; c_i and c_f are the polymer concentrations before and after adsorption, respectively; and V is the volume of the suspension. The error bars included in isotherm plots were calculated at 95% confidence interval from the propagation of errors relating to three replicate solution concentration determinations at a given pH.

2.2.3. Zeta potential measurements

Dilute (i.e., 0.5 wt.% solid) sericite or chalcocite suspensions were prepared in 0.01 M KNO_3 electrolyte solution, and homogenized by magnetic stirring for 30 min at a desired pH. 1 g dm^3 stock Cyquest 3223 and P80 polymer solutions in 0.01 M KNO_3 were prepared and also homogenized by magnetic stirring at the pristine pH 8.7 and 3.4, respectively, overnight. Prior to use, the Cyquest 3223 or P80 polymer solution's pH was adjusted to a desired value and magnetically stirred for 30 min. A known amount of the mineral suspension was mixed with a required volume of polymer solutions at various dosages for particle zeta potential analysis. The dispersion pH was re-adjusted to the desired value and agitated for 30 min by a rotary mixer. It was then allowed to stand for 5 min where the suspended colloidal particles (<5 μm in size) were siphoned off for zeta potential measurement. The zeta potential measurements were performed on more dilute (~0.05 wt.% solid) sericite and chalcocite suspensions using the Nano-ZS Zetasizer (Malvern Instruments Ltd., Worcestershire, U.K.) in electrophoretic light scattering mode with a disposable capillary cell at 23 °C. The recorded particle zeta potentials showed good reproducibility within ±2.5 mV standard deviation estimated at 95% confidence level.

2.2.4. Dissolved Cu(II) species and their effect on polymer uptake

In earlier studies, we showed that Cu(II) species leached from chalcocite particles into solution, the extent of which increased with decreasing pH and increasing time. The concentrations of Cu species leached into solution from the chalcocite particles were determined in the presence and absence of the Cyquest 3223 and P80 polymeric dispersants as a function of time and suspension pH by the inductively coupled plasma (ICP) method [12,31]. The ramifications of the leached Cu species on particle interactions and electrokinetic potentials [12] and polymer adsorption behaviour [31] are brought to bear in the present polymer-mediated chalcocite dispersion stabilization work.

2.2.5. Suspension rheology

Individual sericite or chalcocite particle interactions were characterized by the rheological behaviour of their concentrated slurries. Attempts were made to use the vane technique to directly measure all the shear yield stresses for both sericite and chalcocite dispersions, but they were aborted as the yield values obtained in most cases were well below the acceptable lower limit (i.e., 20 Pa) [20,21]. Hence, measurements were made using the Couette concentric cylinder rheometer (Haake RotoVisco RV1, Thermo Electron GmbH, Germany) with a rotating inner cylinder Z34 DIN rotor and a stationary outer cylinder Z43 measuring cup with a gap width of 1.5 mm. The concentric cylinder technique enables dispersion flow curve analysis and the estimation of extrapolated yield values. The complete details of rheological analysis are given in Ref. [12]. Rheological measurement for each slurry sample was replicated at least three times at 23 °C and the mean values of shear stress; shear rate and viscosity were used for further analysis. The measured flow curves showed time-independent, non-Newtonian, Bingham plastic behaviour. Preliminary analysis indicated that the simple, two-parameter Casson model (Eq. (2)) is more suitable than the Bingham model for fitting the curves at shear rates <200 s^{-1} to obtain an extrapolated shear yield stress. The latter was found to overestimate the true shear yield value more than the former [12,22,23].

$$\tau^{1/2} = (\tau_C)^{1/2} + (\eta_C \gamma)^{1/2} \quad (2)$$

where τ (Pa) is the shear stress, γ (s^{-1}) is the shear rate, τ_C (Pa) is the yield stress, and η_C (Pa s) is the viscosity term.

Further analysis of the particle interactions reflected by the dispersion shear yield stress was performed using the particle interaction model [12,24–26]. The model considers only the contributions of the van der Waals and electrical double layer interactions to the total particle interaction energy potential, as described by the DLVO theory [27,28]. The net particle interaction forces are simply described by the suspension yield stress as shown in Eq. (3) [26]:

$$\tau_0 = \tau_{0,\max} - k_y \zeta^2 \quad (3)$$

where τ_0 is the measured shear yield stress (Pa), ζ is the particle zeta potential (V), and k_y is a constant, and $\tau_{0,\max}$ is the maximum value of the shear yield stress (Pa) observed at the isoelectric point (iep) of the particles and corresponds to the attractive van der Waals interactions whilst the second term denotes repulsive electrical double layer interactions.

3. Results

3.1. Particulate and polymer adsorption

Typical microscopic images captured *in situ* during continuous flow of 3.5 wt.% solid sericite suspension metered past a planar chalcocite surface at pH 5, 7 and 9 are shown in Fig. 2(b), (c) and (d), respectively. It is shown that a lower pH leads to a higher propensity of sericite particles proliferation at chalcocite planar surface. Comparison of the images with that of the baseline (Fig. 2(a)) clearly demonstrates that significant hetero-aggregation between sericite and chalcocite occurred, consistent with our previous studies [12].

Fig. 3(a) and (b), respectively, shows the adsorbed Cyquest 3223 and P80 polymer densities onto sericite particles as a function of the polymer concentration at pH 5, 7 and 9. A marked pH effect on the adsorption affinity and plateau values of both polymers onto sericite is evident. Plateau adsorption occurs at dosages >3 g polymer kg^{-1} solid at all three pH values for both polymers. For the carboxylate-functionalized Cyquest 3223 polymer, this leads to ~0.23, 0.18 and 0.14 mg m^{-2} adsorbed plateau densities, respectively at pH 5, 7 and 9. The polymer adsorption affinity observed at dosages <~1.5 g kg^{-1} solid, however, was pH-independent. Cyquest 3223 polymer has a pKa of 4.2, hence its degree of dissociation is lower at pH 5 than at pH 7 and 9. The polymer appears to adsorb

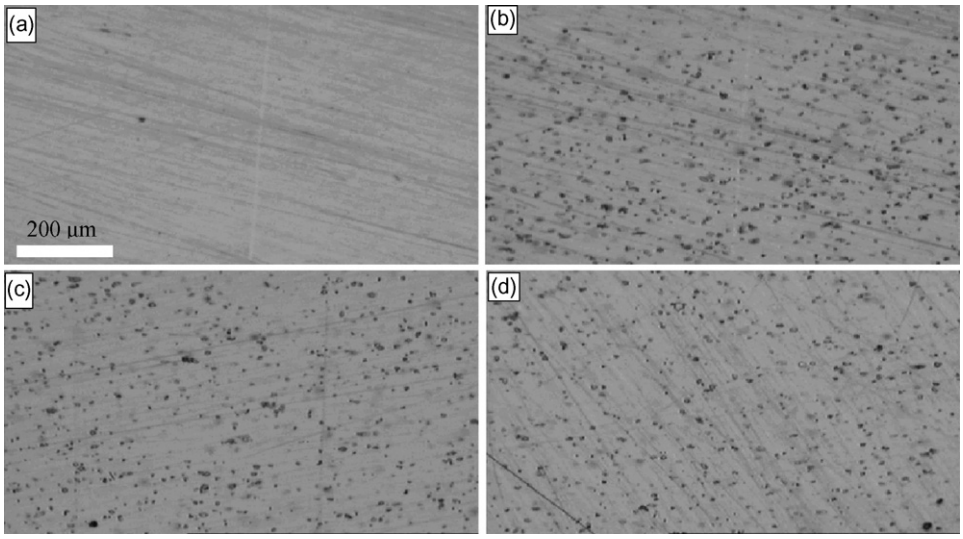

Fig. 2. Images showing sericite particle adsorption onto flat chalcocite surface in 0.01 M KNO_3 electrolyte solution: (a) initial chalcocite planar surface exposed to sericite-free solution (prior to particulate adsorption) and after 15 min of exposure to 3.5 wt.% solid sericite suspensions at (b) pH 5, (c) pH 7 and (d) pH 9 under air-saturation (lateral size/scale: 1.0 mm × 0.6 mm).

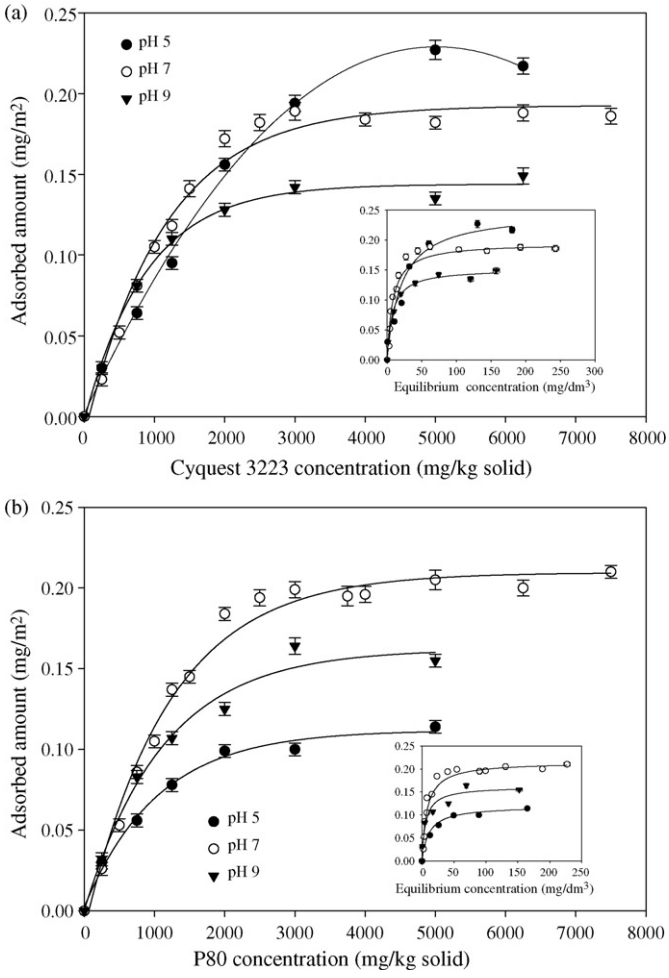

Fig. 3. Cyquest 3223 (a) and P80 (b) polymer adsorption onto sericite as a function of concentration at three pH values in 0.01 M KNO_3 solution. Insert: adsorbed polymer density versus polymer equilibrium solution concentration.

more onto the negatively charged sericite surface at pH 5 where electrostatically repulsive interactions are minimum, in contrast to pH 7 and 9, resulting in a higher plateau adsorption density.

As a distinct difference from Cyquest 3223 polymer adsorption onto sericite, a pronounced pH and dosage effect are evident for both P80 polymer adsorption affinity and plateau density (Fig. 3(b)). P80 displays the highest affinity and largest plateau density at pH 7, followed by pH 9 and 5 in that order. Furthermore, whilst the plateau adsorption density of Cyquest 3223 was greater at pH 5 than at pH 7, P80 shows a considerably higher plateau density at pH 7 than at pH 5. P80 polymer adsorption propensity being greater at pH 7 than at pH 9 and 5 may be rationalized in terms of the balance between pH-dependent degree of dissociation and electrostatically repulsive interactions, both of which increase with increasing pH. Whilst electrical double layer effect seems to limit the adsorption of the larger molecular weight Cyquest 3223 polymer (26,000 Da) at higher than at lower pH, it does not appear to be the cause for the lower molecular weight P80 polymer (8500 Da). It is, however, not clear exactly how the differences in polymer molecular weight and functionality influence the adsorption process at various pH values.

Cyquest 3223 and P80 polymer adsorption onto chalcocite as a function of polymer concentration at pH 5, 7 and 9 is plotted in Fig. 4(a) and (b), respectively. The adsorption affinities and plateau densities of both polymers onto chalcocite are dramatically increased over those of sericite. Furthermore, the adsorption behaviour is quite similar at pH 7 and 9 for both polymers, with plateau coverage attained at dosages >1 g kg^{-1} solid and P80 displaying ~40% higher plateau density than Cyquest 3223. At pH 5, however, both P80 and Cyquest 3223 polymers show similar, extremely high affinities onto chalcocite surface without reaching a plateau. The adsorbed polymer density increases monotonically with increasing polymer concentration, indicating that all the added polymers are substantially and progressively removed from solution. This unlimited adsorption behaviour at pH 5 is unusually ascribed to the mediation of high concentration of Cu(II) species which leached in the chalcocite suspension at pH 5 [12]. The lower adsorption propensities at pH 7 and 9 are consistent with significantly reduced Cu(II) ions leached from chalcocite at these two pH values.

It has been shown that under air-saturation conditions at 23 °C, 6.16×10^{-3} M Cu(II) species leached from a similar 3.5 wt.% solid chalcocite dispersion at pH 5 in 2 h [12]. These

Cu(II) species have been reported to strongly interact with poly(acrylic acid) and poly(acrylamide) polymers in aqueous systems [29–31]. Cyquest 3223 and P80 polymers containing carboxylate–primary amide and carboxyl–sulphonate functional groups, respectively, may strongly interact with the Cu(II) species leached from chalcocite or exposed at its surfaces. For optically clear, 6.16×10^{-3} M Cu(II) solutions at pH 5, the residual Cu(II) species decreased linearly with increasing Cyquest 3223 polymer concentration but was invariant with P80 dosage [31]. A green precipitate, indicative of insoluble Cu(II)–polymer complex formation, was visually observed in the Cyquest 3223 treated solution. Precipitation leads to simultaneous removal of both the polymer and Cu(II) species from solution. Furthermore, upon the addition of the polymers to 3.5 wt.% solid chalcocite suspensions dispersed at pH 5 in 2.2×10^{-3} M Cu(II), supernatant Cu concentration decreased monotonically with increasing polymer concentration [31]. Thus, it appears that the polymers' interactions with Cu(II) species in the presence of chalcocite particles facilitate a strong Cu(II)–polymer complex adsorption.

3.2. Electrokinetic zeta potential

Fig. 5(a) and (b) shows the zeta potential of sericite particles as a function of Cyquest 3223 and P80 polymer concentrations, respectively, dispersed in 0.01 M KNO_3 solution at pH 5, 7 and 9. The zeta potential of pristine sericite particles at zero polymer concentration is strongly pH-dependent and negative, ranging from −30 to −48 mV. Following the anionic polymers addition, the magnitude of the particle zeta potential increases more rapidly at pH 5 than at pH 7 and 9 with increasing polymer concentration up to 2 g polymer kg^{-1} solid. This observation is inconsistent with the adsorption isotherm data (Fig. 3), which indicate pH-independent polymer adsorption at concentrations <2 g kg^{-1} solid for Cyquest 3223, and lowest adsorption density at pH 5 for P80 at all dosages. At pH 7 and 9, similar sericite particle zeta potentials are observed in the presence of both polymers. A noticeable, abrupt decrease followed by slight increase in the magnitude of the zeta potential is observed at dosages between 0 and 1 g polymer kg^{-1} solid.

At pH 5, both Cyquest 3223 and P80 polymers are ~70% charged and may, therefore, not fully display expanded interfacial conformations. The polymers are, however, completely dissociated and fully anionically charged at pH > 7 [31,32] where a maximum expanded conformation at the negatively charged sericite surfaces

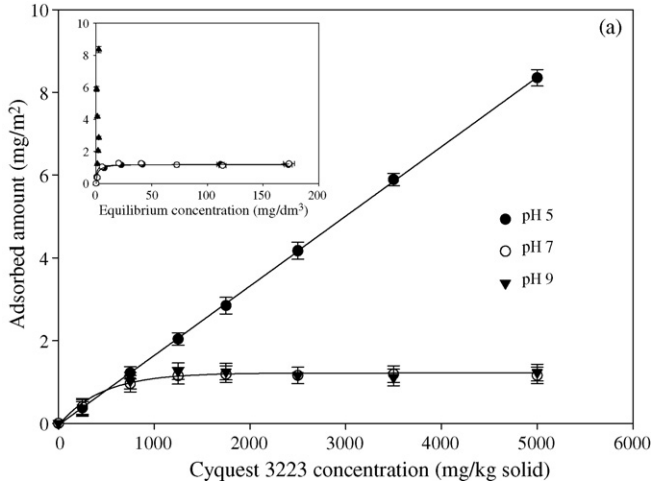

Fig. 4. Cyquest 3223 polymer adsorption onto chalcocite as a function of concentration at three pH values in 0.01 M KNO_3 solution. Insert: adsorbed polymer density versus polymer equilibrium solution concentration. Similar adsorption behaviour was displayed by P80 polymer.

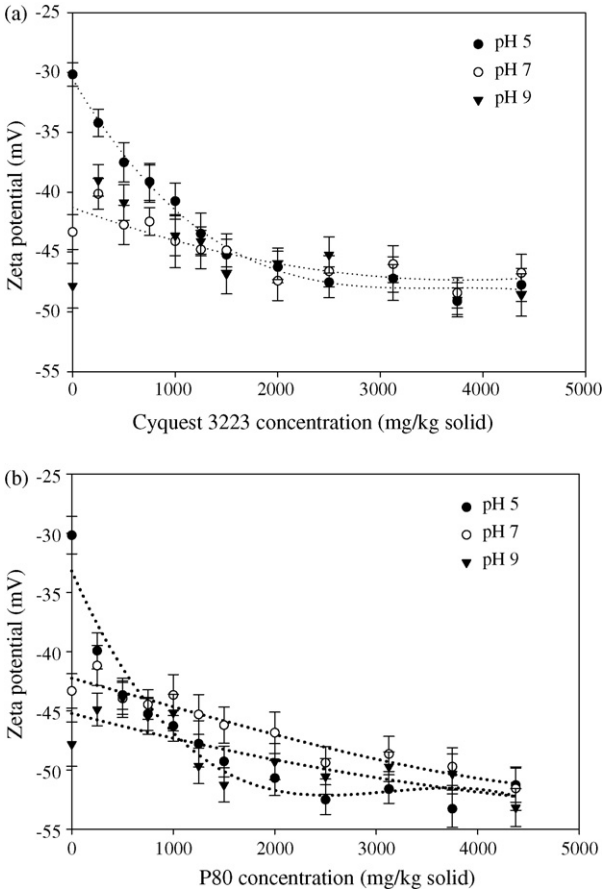

Fig. 5. Zeta potential of sericite particles dispersed in 0.01 M KNO_3 solution as a function of Cyquest 3223 (a) and P80 (b) polymer concentrations at three pH values.

can be expected. The adsorption of the anionically charged polymer not only increases the particle surface charge but also shifts the shear plane away from the surface. The shear plane shift, however, leads to a reduction in the magnitude of particle zeta potential. Seemingly at pH 5, the increase in surface charge due to the less expanded polymer adsorption predominates the reduction in the magnitude of particle zeta potential due to the shift of the shear plane.

At pH 7 and 9, shear plane shift due to adsorbed polymer at low dosages leads to a greater reduction in the magnitude of the zeta potential than the increase resulting from surface charging effect. This results in an abrupt decrease in the magnitude of the zeta potential. At higher dosages (>1 g kg^{-1} solid), however, the reverse is true. A marked increase in surface charge due to the proliferation of adsorbed anionic polymer chains supersedes the decrease in the magnitude of zeta potential due to the shear plane shift. Hence, in the absence of strong electrical double layer compression effect, the magnitude of the zeta potential slightly increases at polymer dosages up to 2 g kg^{-1} solid. It is pertinent to note that the marked variations in the adsorbed polymer density at dosages >2 g kg^{-1} solid due to pH (Fig. 3) have an insignificant impact on the resulting particle zeta potential, which plateaus at approximately −48 and −52 mV, respectively, for Cyquest 3223 and P80 polymers, regardless of the pH (Fig. 6). This indicates that the adsorbed polymer layer dominates the sericite particle interfacial chemistry at >75% plateau adsorption density.

The chalcocite particle zeta potential as a function of Cyquest 3223 and P80 polymer concentrations at pH 5, 7, and 9 in 0.01 M KNO_3 solution is plotted in Fig. 7(a) and (b), respectively. The zeta potential shows marked pH and polymer concentration dependen-

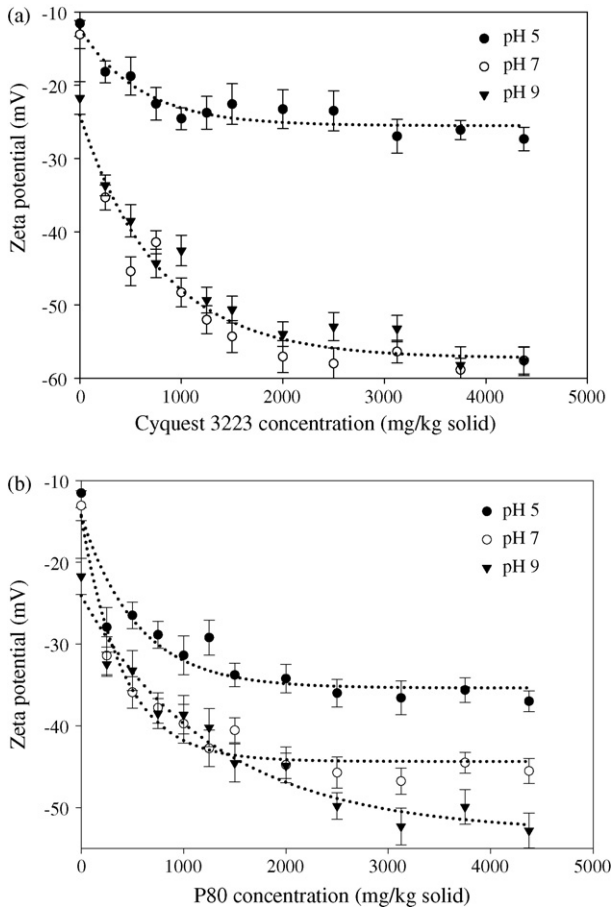

Fig. 6. Zeta potential of chalcocite particles as a function of Cyquest 3223 (a) and P80 (b) polymer concentrations at three pH values in 0.01 M KNO_3 background solution.

cies. At pH 5, the magnitude of the zeta potential increases by more than 100% from the initial value of approximately −11.5 to −23 and −32 mV, respectively, for Cyquest 3223 and P80 at polymer concentration 1 g kg^{-1} solid. Although both polymers display substantially the same adsorption behaviour at pH 5 (Fig. 4(a) and (b)), there is a noticeable impact of polymer structure type on the resulting zeta potential. At polymer dosages >2 g kg^{-1} solid which leads close to plateau adsorption, the increase in the magnitude of particle zeta potential is ∼40% higher for P80 than for Cyquest 3223. On the other hand, a similar polymer effect on the particle zeta potential is observed at pH 7 and 9, consistent with the adsorption behaviour (Fig. 4). The magnitude of the particle zeta potential remains constant upon increasing polymer concentration above 2 g kg^{-1} solid at all pH values. It is pertinent to note that, although 100% polymer adsorption occurs at pH 5 (Fig. 4), the concomitant increase in the magnitude of particle zeta potential is significantly lower than those at pH 7 and 9, particularly for the Cyquest 3223 polymer.

This observation, which is contrary to the adsorption density data, may be ascribed to pH-mediated chalcocite oxidation and Cu(II) leach effect, impacting on the interfacial chemistry. The leaching of Cu(II) species from chalcocite particles is significantly greater at pH 5 than at pH 7 and 9, where 6.16×10^{-3}, 1.11×10^{-4} and 2.7×10^{-5} M Cu(II) ion were, respectively, observed in solution within 2 h [12]. The dissolved, electropositive Cu(II) species interactions with the anionic functional groups of both polymer molecules would result in charge neutralization. Both Cyquest 3223 and P80 polymers are ∼70% and 100% charged at pH 5 and >7, respectively [31]. The higher Cu(II) ion concentration and lower polymer charge, therefore, appear to largely account for the smaller increase in the magnitude of the particle zeta potential at pH 5. Furthermore, one may not completely discount the effect of electrical double layer compression due to the higher concentration of leached Cu(II) species which prevails at pH 5. For the P80 polymer, a small but noticeable difference in the magnitudes of the zeta potentials at dosages >2 g kg^{-1} solid for pH 7 and 9 is indicated. This is consistent with the Cu(II) species leach effect. Generally speaking, no simple correlation between the pH-mediated adsorbed polymer properties and the resulting particle zeta potential may be drawn. Clear pH, polymer structure type and concentration, and mineral phase specific relationships are, however, apparent and in some cases, they are counter-intuitive.

3.3. Suspension rheology

Figs. 7 and 8 show the effect of Cyquest 3223 and P80 polymer dosages and shear rate on the rheological behaviour of 40 wt.% solid (19.2 vol%) sericite slurry in 0.01 M KNO_3 solution at pH 5 at 23 °C. The slurries display a non-Newtonian, Bingham plastic behaviour at polymer dosages up to 3 g kg^{-1} solid. In the presence of the polymer, the shear stress at a given shear rate decreases non-linearly with increasing polymer concentration, consistent with the expectation based on the zeta potential data shown in Fig. 6. The data in Fig. 7 indicate that the sericite dispersion's yield value that may be extrapolated from the curve at 0 shear rate is substantially the same and negligibly small at polymer dosages >1.5 g kg^{-1} solid. Similar rheological trends were shown by 75 wt.% solid (34.7 vol%) chalcocite dispersions. Fig. 8(a) shows that the rheology of 40 wt.% solid sericite dispersion is pH independent whilst Fig. 8(b), on the other hand, it also polymer structure type-independent at polymer dosages of 1.0 and 1.5–3.0 g kg^{-1} solid.

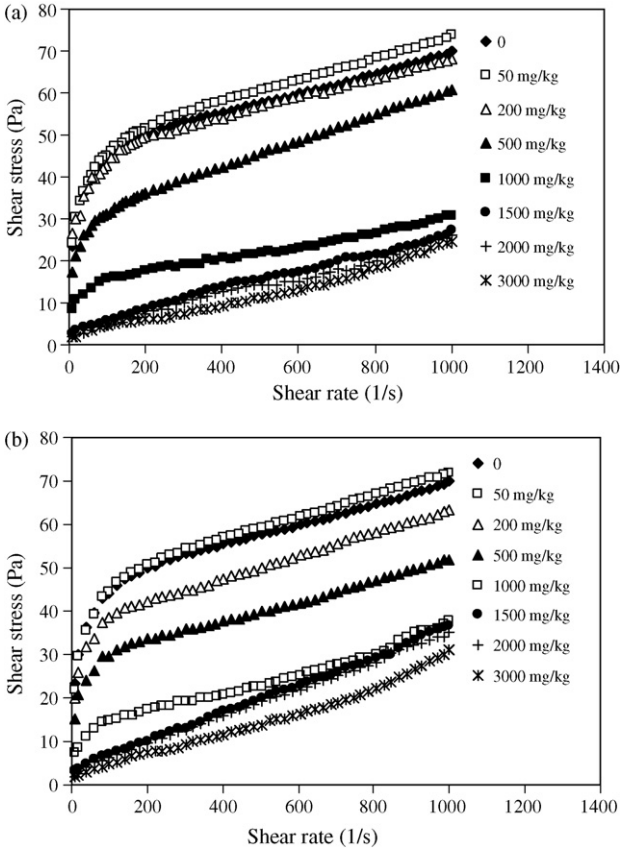

Fig. 7. Effect of polymer Cyquest 3223 (a) and P80 (b) concentration on the sericite slurry rheology at 40 wt.% solid concentration in 10^{-2} KNO_3 solution at pH 5.

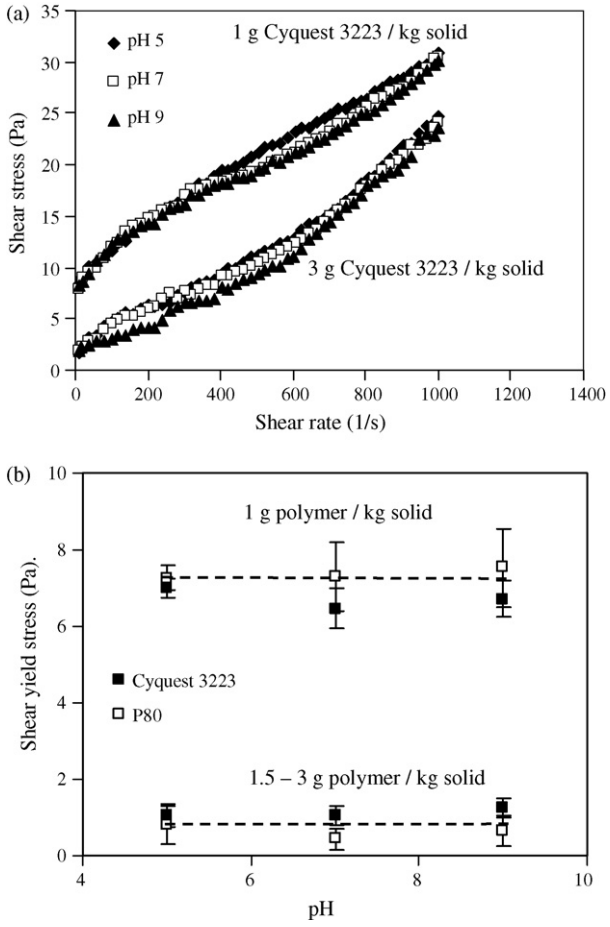

Fig. 8. Effect of pH on the flow curves (a) and shear yield stress (b) for 40 wt.% solid sericite slurry in the presence of 1 g and 3 g Cyquest 3223 $kg^{(1}$ solid in 0.01 M KNO_3 electrolyte at 23 °C.

The extrapolated Casson shear yield stresses of 40 wt.% sericite dispersion at pH 5 and 75 wt.% solid chalcocite dispersions at pH 5 and 9 are shown in Fig. 9, as a function of Cyquest 3223 or P80 polymer concentrations. The shear yield stress of the sericite dispersion at pH 5, which initially was higher than that of chalcocite, decreased in a distinctly exponential manner with increasing polymer concentration and is independent of polymer functionality type. The yield stresses of chalcocite dispersions were higher at pH 5 than at pH 9 or greater at lower than higher polymer dosage as expected, except at 500 g Cyquest kg^{-1} solid where a noticeable enhancement is observed. Excepting the data at 500 g polymer kg^{-1} solid, both polymers exhibit substantially similar dispersing ability in reducing shear yield stress at a given pH. The abrupt increase in chalcocite dispersion yield stress at pH 5 in the presence of 500 g Cyquest kg^{-1} solid may be attributed to strong, synergistic particle interactions arising from polymer functionality-specific Cu(II) complexation action. Solution Cu(II)–Cyquest 3223 polymer complex-based green precipitate has been observed to form at pH 5 but not in the case of P80 [31]. Particle cementation action of such Cu(II)–Cyquest 3223 polymer complex deposited in dispersion may lead to attractive coagulation and particle bridging forces which are stronger than the prevailing electrical double layer repulsion. Interestingly, it is noted that Cyquest 3223 polymer addition results in 40% lower increase in the magnitude of chalcocite particle zeta potential than P80 polymer in the dosage range of 1–3 g kg^{-1} solid at pH 5 (Fig. 6), where similar yield values are observed. This implies that polymer-induced, repulsive steric particle interactions play a major role in the mechanism underpinning dispersing. Adsorbed polymer layer coverage and interfacial conformation are expected to play a pivotal role in the electro-steric mechanism.

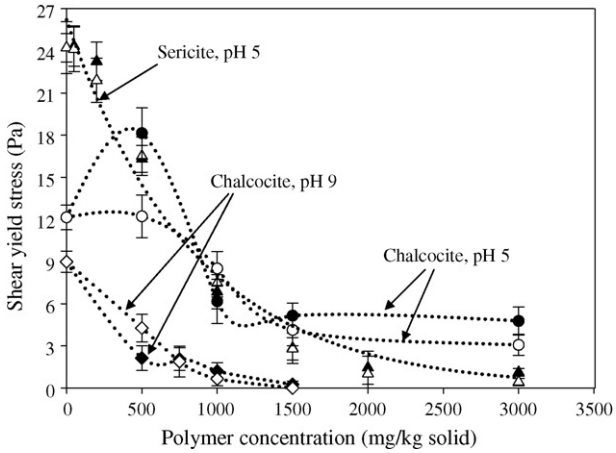

Fig. 9. Shear yield stress as a function of Cyquest 3223 and P80 polymer concentration for 40 wt.% solid (19.2 vol%) sericite dispersion at pH 5 and 75 wt.% solid (34.7 vol%) chalcocite dispersion at pH 5 and 9 in 0.01 M KNO_3 solution at 23 °C. Filled and unfilled symbols refer to Cyquest 3223 and P80 polymers, respectively.

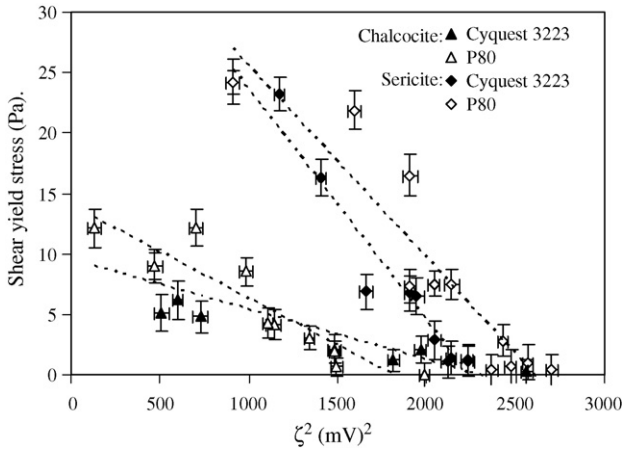

Fig. 10. Casson yield stress as a function of the square of zeta potential for 40 wt.% solid sericite and 75 wt.% solid chalcocite particles dispersed in 0.01 M KNO_3 solution in the presence and absence of polymer at different pH values at 23 °C.

Further analysis of the particle interactions reflected by the dispersions' shear yield stresses is performed using the particle interaction model [26], which allows the net particle interaction forces to be described by the suspension shear yield stress. The plot of the shear yield stress against the square of the particle zeta potential in the pH range 5–9 deviates from linearity and hence, DLVO theory for the individual sericite and chalcocite pulps in the presence of Cyquest 3223 or P80 polymer (Fig. 10). This is more apparent at the square of the zeta potential >1700 $(mV)^2$, corresponding to polymer plateau adsorption. Non-DLVO repulsive steric forces are implicated due to the bulk presence of adsorbed polymer layer at a high coverage on the particles' surfaces. The data scatter may be attributed to polymer structure/pH-dependent variations in zeta potential, interfacial conformations and the relative contributions of electrostatic and steric forces.

Fig. 11 provides visual information on the effect of the two polymeric dispersants on sericite particulate adsorption onto a chalcocite planar surface at pH 5. The quantification of the extent of sericite particle coverage on chalcocite surface (% area) at pH 5 and 9 is summarized in Fig. 12. As can be seen from the data, the propensity of sericite adsorption onto chalcocite surface is significantly

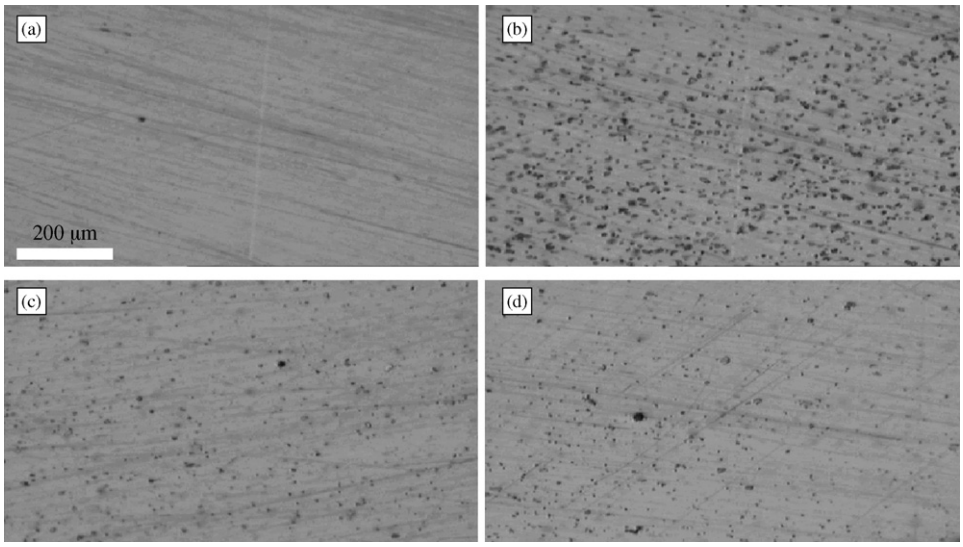

Fig. 11. Images showing sericite particle adsorption onto flat chalcocite surface at pH 5 in 0.01 M KNO_3 electrolyte solution: (a) bare chalcocite particle surface before adsorption and after 30 min of exposure to 3.5 wt.% solid sericite suspensions (b) in the absence of polymer, (c) in the presence of 3 g polymer Cyquest 3223 kg^{-1} solid and (d) in the presence of 3 g P80 polymer kg^{-1} solid (lateral scale: 1.0 mm × 0.6 mm).

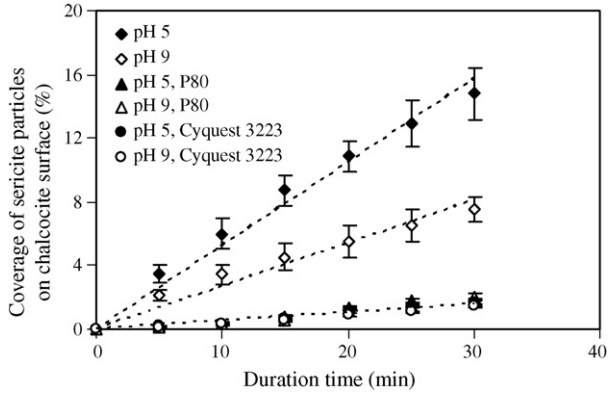

Fig. 12. Effect of pH and polymer Cyquest 3223 or P80 addition on the sericite particle adsorption density onto chalcocite surface at 3.5 wt.% solid sericite suspension in the presence of 3 g polymer kg^{-1} solid in 0.01 M KNO_3 solution.

higher at pH 5 than at pH 9 in the absence of a dispersant. The addition of Cyquest 3223 or P80 polymer at 3 g kg^{-1} solid dosage almost completely eliminates the sliming of sericite onto chalcocite.

4. Discussion

Both Cyquest 3223 and P80 polymers show high adsorption affinity onto sericite and chalcocite particles, a behaviour that is dramatically accentuated for the latter particularly at pH 5. This has a pronounced effect on the magnitude of individual mineral particles' zeta potentials and hence, the repulsive particle interactions, reflecting significantly reduced shear yield stresses. The addition of both polymers also leads to a reduction in leached Cu(II) species in chalcocite dispersions (Fig. 5(b)). The chalcocite particles provide active adsorption sites for the Cu(II)–polymer complexes. At pH 5, the specifically adsorbing Cu(II) species leached, create localized patches of electropositive sites at the mineral surface [12]. This together with polymer–Cu(II)–polymer complexes which form may increase the effective molecular weight for polymer adsorption occurring through chemical, electrostatic charge patch attraction and hydrogen bonding mechanisms [29–31]. Furthermore, a higher pH (i.e., pH 9) not only leads to an increase in the magnitude of both sericite and chalcocite particle zeta potentials (Figs. 6 and 7), but also a marked reduction of chalcocite oxidation and leach to form Cu(II) species [12].

These findings clearly show that both high pH and anionic polymer adsorption at plateau coverage lead to prevention of sericite–chalcocite attractive particle interactions, reminiscent of repulsive electrical double layer and sterically stabilized interactions as a result of a dramatic increase in the magnitude of zeta potentials (Figs. 6 and 7) and a high adsorbed polymer density (Figs. 3 and 4) for both sericite and chalcocite particles. The particulate adsorption studies are consistent with both the zeta potential and shear rheology data. For instance, in the presence of 3 g Cyquest 3223 or P80 polymer kg^{-1} solid corresponding to plateau adsorption density (Figs. 3 and 4), the sliming of sericite particles onto chalcocite surfaces is completely prevented, with an insignificant pH effect. This confirms that strong, polymer-induced steric forces prevail in the sericite–chalcocite particle interactions, taking into account the zeta potential differences at different pH values (Fig. 7).

Certainly, a higher polymer dosage leads to a greater increase in the magnitude of the sericite and chalcocite particle zeta potentials and higher adsorbed polymer layer coverage, both of which lead to enhanced, repulsive electro-steric particle interaction, reflecting lower yield stresses. For instance, higher dosages (>1.5 g polymer kg^{-1} solid) lead to plateau adsorption density, inducing both repulsive electrostatic and steric forces to control the mineral particles' interactions (Fig. 9). Both polymers exhibit similar dispersing efficacy in reducing attractive particle interactions for both sericite and chalcocite. Although the adsorbed polymer interfacial conformation was not quantified, it is believed that it plays an important role in the electro-steric mechanism underpinning the dispersing process. Considerably reduced shear yield stresses and significantly suppressed hetero-aggregation (i.e., sliming) between sericite and chalcocite are observed at a high polymer dosage (e.g., >1.5 g kg^{-1} solid).

The polymer dosage range 1.5–3 g kg^{-1} at which both Cyquest 3223 and P80 solid display high efficacy in dispersion stabilization is considered to be cost-effective. Previous polymer-mediated dispersion stabilization studies indicate that polymeric dispersant dosage, dependent upon the mineral particle size and its distribution and/or specific surface area, solid concentration and particle surface chemistry, was in the range of 1–50 g polymer kg^{-1} solid [33–36]. For instance, the addition of 0.1–1 wt.% (~1–10 g kg^{-1} solid) tripolyphosphate or polyphosphate

led to a marked reduction in rheology (i.e., viscosities and storage and loss moduli) of 55 wt.% kaolin (<20 μm) suspension [33]. Huynh et al. [34] reported that the shear yield stresses of 77–79 wt.% solid tailings (comprising magnetite, quartz, chlorite, garnet, hedenbergite, olivine, pyrrhotite) and 74–79 wt.% Portland cement paste were decreased to a minimum or were practically eliminated at polyphosphate or naphthalene sulphonate formaldehyde condensate dosages of >2 g kg^{-1} solid. For TiO_2 pigment particle suspension stabilization, the dispersant dosage was in the range of 0.3–5 wt.% (i.e., 3–50 g kg^{-1} solid), depending upon the particle size and polymer structure type [35,36].

5. Conclusions

The use of low molecular weight, anionic co-polymers (carboxylate- versus sulphonate-substituted) to modify the interfacial chemistry and effectively regulate the particle interactions which underpin hetero-aggregation of negatively charged sericite and chalcocite particles has been demonstrated. Polymer addition led to a marked pH and polymer functionality dependency of polymer adsorption propensity and particle zeta potential except for sericite at polymer dosages >1 g kg^{-1} solid, where the electrokinetic potential is independent of the polymer functionality and the pulp pH. Both polymers showed greater adsorption onto chalcocite, in contrast with sericite, leading to a markedly lower increase in the magnitude of the particle zeta potential at pH 5 than at pH 7 and 9. This observation is ascribed to polymer charge neutralization effect arising from electropositive Cu(II) species leached from chalcocite particle surface. The particulate adsorption and shear rheology studies are highly consistent with zeta potential data. Both polymers were effective at dosages >1.5 g kg^{-1} solid in increasing the magnitude of the particle zeta potential, dramatically reducing the dispersion shear yield stress or suppressing sericite–chalcocite attractive interactions (sliming) via an electro-sterically repulsive mechanism. Cyquest 3223 and P80 polymers show similar high dispersing efficacy for sericite–chalcocite dispersions at high polymer dosages of >1.5 g kg^{-1} solid, regardless of the pH.

Acknowledgements

The financial support provided by the Australian Research Council and P498B (Polymers at Mineral Interfaces) project sponsors, comprising Penford Australia, Cytec, CP Kelco, Xstrata, Rio Tinto, and Anglo Platinum through AMIRA International is gratefully acknowledged. The authors would like to acknowledge the useful discussions provided by Professors John Ralston and Daniel Fornasiero.

References

[1] C.R. Edwards, W.B. Kipkie, G.E. Agar, The effect of sliming coatings of the serpentine minerals, chrysotile and lizardite, on pentlandite flotation, Int. J. Miner. Process. 7 (1980) 33–42.
[2] D. Fornasiero, J. Ralston, Effect of surface oxide/hydroxide products on the collectorless flotation of copper-activated sphalerite, Int. J. Miner. Process. 78 (2006) 231–237.
[3] A.M. Gaudin, D.W. Fuerstenau, H.L. Miaw, Slime-coatings in galena flotation, CIM Bull. 53 (1960) 960–963.
[4] M.E. Learmont, I. Iwasaki, Effect of grinding media on galena flotation, Miner. Metall. Process. 1 (1984) 136–143.
[5] T.K. Mitchell, A.V. Nguyen, G.M. Evans, Heterocoagulation of chalcopyrite and pyrite minerals in flotation separation, Adv. Colloid Interface Sci. 114 (2005) 227–237.
[6] G.D. Senior, W.J. Trahar, The influence of metal hydroxides and collector on the flotation of chalcopyrite, Int. J. Miner. Process. 33 (1991) 321–341.
[7] W.J. Trahar, A rational interpretation of the role of particle size in flotation, Int. J. Miner. Process. 8 (1981) 289–327.
[8] K.E. Bremmell, D. Fornasiero, J. Ralston, Pentlandite–lizardite interactions and implications for their separation by flotation, Colloids Surf. A 252 (2005) 207–212.
[9] G. Chen, S. Grano, S. Sobieraj, J. Ralston, The effect of high intensity conditioning on the flotation of a nickel ore: Part 1: size-by-size analysis, Miner. Eng. 12 (1999) 1185–1200.
[10] G. Chen, S. Grano, S. Sobieraj, J. Ralston, The effect of high intensity conditioning on the flotation of a nickel ore: Part 2: mechanisms, Miner. Eng. 12 (1999) 1359–1373.
[11] L. Huynh, A. Feiler, A. Michelmore, J. Ralston, P. Jenkins, Control of slime coatings by the use of anionic phosphates: a fundamental study, Miner. Eng. 13 (2000) 1059–1069.
[12] M. He, J. Addai-Mensah, D. Beattie, Sericite–chalcocite mineral particle interactions and hetero-aggregation (sliming) mechanism in aqueous media, Chem. Eng. Sci. 64 (2009) 3083–3093.
[13] S. Song, A. Lopez-Valdivieso, C. Martinez-Martinez, R. Torres-Armenta, Improving fluorite flotation from ores by dispersion processing, Miner. Eng. 19 (2006) 912–917.
[14] Q. Wang, K. Heiskanen, Dispersion selectivity and heterocoagulation in apatite–hematite–phlogopite fine particle suspensions. II. Dispersion selectivities of the mineral mixtures, Int. J. Miner. Process. 35 (1992) 133–145.
[15] D. Fullston, D. Fornasiero, J. Ralston, Zeta potential study of the oxidation of copper sulphide minerals, Colloids Surf. A 146 (1999) 113–121.
[16] M. Sato, Oxidation of sulfide ore bodies: II. Oxidation mechanisms of sulfide minerals at 25 °C, Econ. Geol. 55 (1960) 1202–1231.
[17] G.W. Walker, J.V. Stout III, P.E. Richardson, Electrochemical flotation of sulfides: reactions of chalcocite in aqueous solution, Int. J. Miner. Process. 12 (1984) 55–72.
[18] M. Dubois, K.A. Gilles, J.K. Hamilton, P.A. Rebers, F. Smith, Colorimetric method for determination of sugars and related substances, Anal. Chem. 28 (1956) 350–356.
[19] M.W. Scoggins, J.W. Miller, Spectrophotometric determination of water soluble organic amides, Anal. Chem. 47 (1975) 152–154.
[20] H.A. Barnes, Q.D. Nguyen, Rotating vane rheometry—a review, J. Non-Newtonian Fluid Mech. 98 (2001) 1–14.
[21] Q.D. Nguyen, D.V. Boger, Yield stress measurement for concentrated suspensions, J. Rheol. 27 (1983) 321–349.
[22] M. He, E. Forssberg, Rheological behaviors in wet ultrafine grinding of limestone, Miner. Metall. Process. 24 (2007) 19–29.
[23] J. Yue, B. Klein, Influence of rheology on the performance of horizontal stirred mills, Miner. Eng. 17 (2004) 1169–1177.
[24] J. Addai-Mensah, J. Ralston, Interfacial chemistry and particle interactions and their impact upon the dewatering behaviour of iron oxide dispersions, Hydrometallurgy 74 (2004) 221–231.
[25] A. McFarlane, K. Bremmell, J. Addai-Mensah, Microstructure, rheology and dewatering behaviour of smectite dispersions during orthokinetic flocculation, Miner. Eng. 18 (2005) 1173–1182.
[26] P.J. Scales, S.B. Johnson, T.W. Healy, P.C. Kapur, Shear yield stress of partially flocculated colloidal suspensions, AIChE J. 44 (1998) 538–544.
[27] B.V. Derjaguin, L.D. Landau, A theory of the stability of strongly charged lyophobic sols and of the adhesion of strongly charged particles in solutions of electrolytes, Acta Physicochim. URSS 14 (1941) 633–662.
[28] E.J.W. Verwey, J.Th.G. Overbeek, Theory of the Stability of Lyophobic Colloids, Elsevier, Amsterdam, The Netherlands, 1948.
[29] G.A. Mun, Z.S. Nurkeeva, V.V. Khutoryanskiy, G.S. Sarybayeva, A.V. Dubolazov, pH-effects in the complex formation of polymers. I. Interaction of poly(acrylic acid) with poly(acrylamide), Eur. Polym. J. 39 (2003) 1687–1691.
[30] R. Subramanian, P. Natarajan, Interaction between poly(N-vinylpyrrolidone) and poly(acrylic acid)s: influence of hydrogen and cupric ions on the adduct formation, J. Polym. Sci. 22 (1984) 437–451.
[31] M. He, J. Addai-Mensah, D. Beattie, The influence of solution conditions and polymer structure type on dispersant adsorption onto chalcocite particles, J. Colloids Interface Sci., submitted for publication.
[32] M. He, J. Addai-Mensah, D. Beattie, Anionic polymer adsorption behaviour at muscovite mica surfaces, Langmuir, in preparation.
[33] A. Papo, L. Piani, R. Ricceri, Sodium tripolyphosphate and polyphosphate as dispersing agents for kaolin suspensions: rheological characterization, Colloids Surf. A 201 (2002) 219–230.
[34] L. Huynh, D.A. Beattie, D. Fornasiero, J. Ralston, Effect of polyphosphate and naphthalene sulphonate formaldehyde condensate on the rheological properties of dewatered tailings and cemented paste backfill, Miner. Eng. 19 (2006) 28–36.
[35] S. Farrokhpay, G. Morris, D. Fornasiero, P. Self, Influence of polymer functional group architecture on titania pigment dispersion, Colloids Surf. A 253 (2005) 183–191.
[36] S.N. Kumari, D. Agarwal, D. Nigam, Synthesis and characterization of alkali-modified styrene–maleic anhydride copolymer for dispersion of TiO_2, J. Appl. Polym. Sci. 103 (2007) 3194–3205.